

Efficient detection of Cr^{3+} and $\text{Cr}_2\text{O}_7^{2-}$ based on a Zn(II) luminescent metal–organic framework

Qi Guo,^[a] Tingting Ma,^[a] Liuqing Zhou,^[b] Jing-xin Ma,^{*[a]} Jinhui Yang,^[a] and Qingfeng Yang^[a]

^a State Key Laboratory of High-efficiency Utilization of Coal and Green Chemical Engineering, National Demonstration Center for Experimental Chemistry Education, College of Chemistry and Chemical Engineering, Ningxia University, Yinchuan 750021, China

^b Department of Otorhinolaryngology, People's Hospital of Ningxia Hui Autonomous Region, Yinchuan 750002, China

Table S1 Selected Bond Distances (Å) and Angles(°) of **1**

Bond Distances	
Zn1-O4	2.021(4)
Zn1-O6	2.000(5)
Zn1-O4a	2.021(4)
Zn1-O1b	2.022(4)
Zn1-O1c	2.022(4)
Zn2-O3	2.014(4)
Zn2-O5	1.995(6)
Zn2-O3a	2.014(4)
Zn2-O2b	2.015(4)
Zn2-O2c	2.015(4)

Bond Angles	
O4-Zn1-O6	99.35(18)
O4-Zn1-O4a	86.9(2)
O1b -Zn1-O4	87.0(2)
O1c-Zn1-O4	158.43(19)
O4a-Zn1-O6	99.35(18)
O1b-Zn1-O6	102.05(17)
O1c-Zn1-O6	102.05(17)
O1b-Zn1-O4a	158.43(19)
O1c-Zn1-O4a	87.0(2)
O1b-Zn1-O1c	91.2(2)
O3-Zn2-O5	103.4(2)
O3-Zn2-O3a	87.4(2)
O2b -Zn2-O3	87.2(2)
O2c-Zn2-O3	156.98(19)
O3a-Zn2-O5	103.4(2)
O2b-Zn2-O5	99.6(2)
O2c-Zn2-O5	99.6(2)
O2b-Zn2-O3a	156.98(19)
O2c-Zn2-O3a	87.2(2)
O2b-Zn2-O2c	89.0(2)

Symmetry transformations used to generate equivalent atoms: a= y, x, z; b= 1/2-y, -1/2+x, 1/2-z; c= -1/2+x, 1/2-y, 1/2-z.

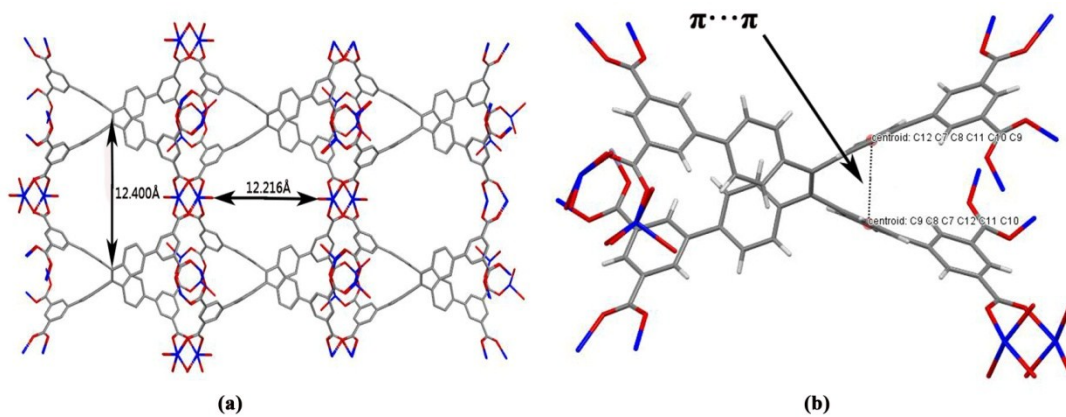


Fig. S1 (a) The pore size of **1** (C: grey, Zn: blue, O: red, H is omitted for clarity); (b) π - π stacking in **1** (C: grey, Zn: blue, O: red, H: white).

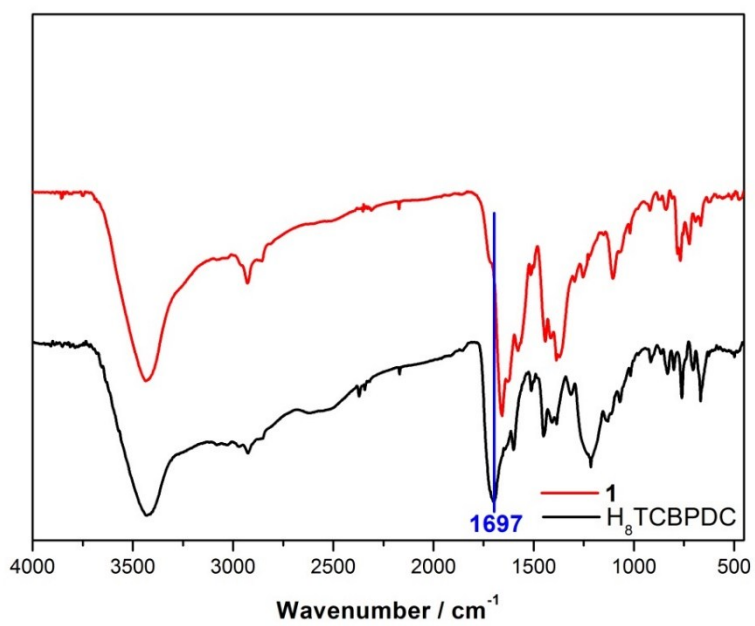


Fig. S2 IR spectrum of **1** and free H_8TCBPDC .

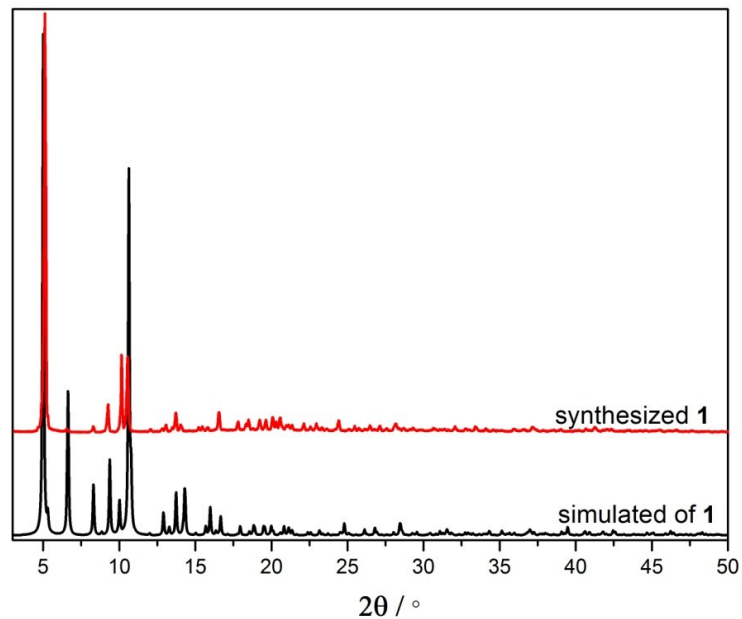


Fig. S3 PXRD patterns of **1** for simulated (black) and the as-synthesized (red).

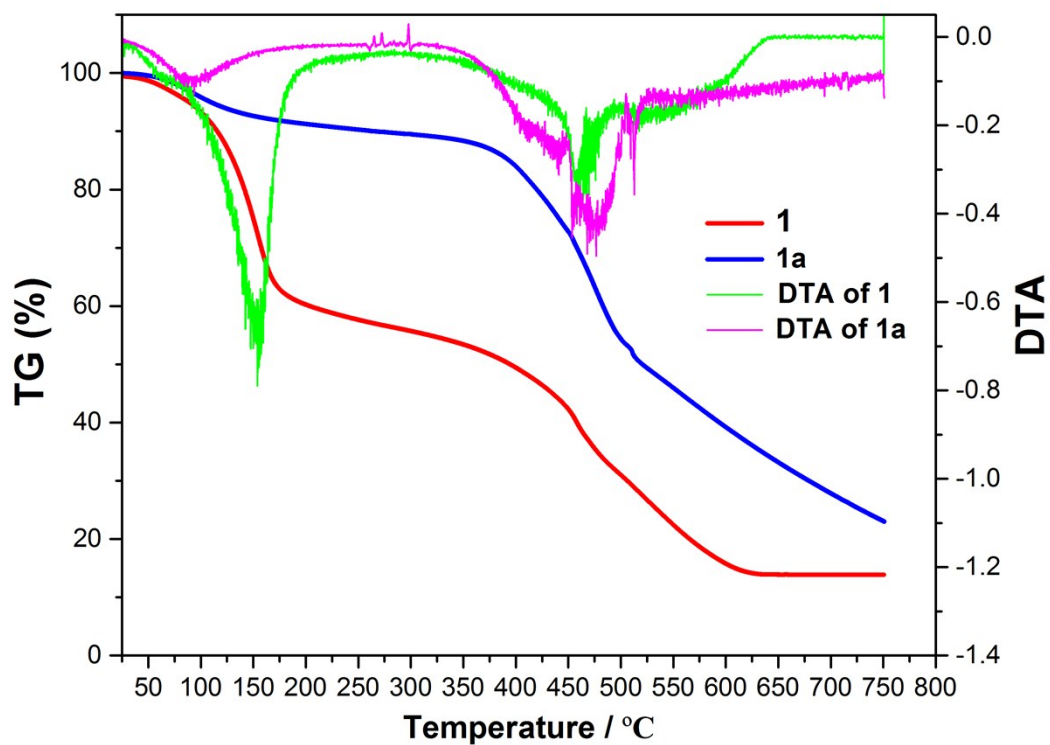


Fig. S4 The TG and DTA curves of **1a** and **1**.

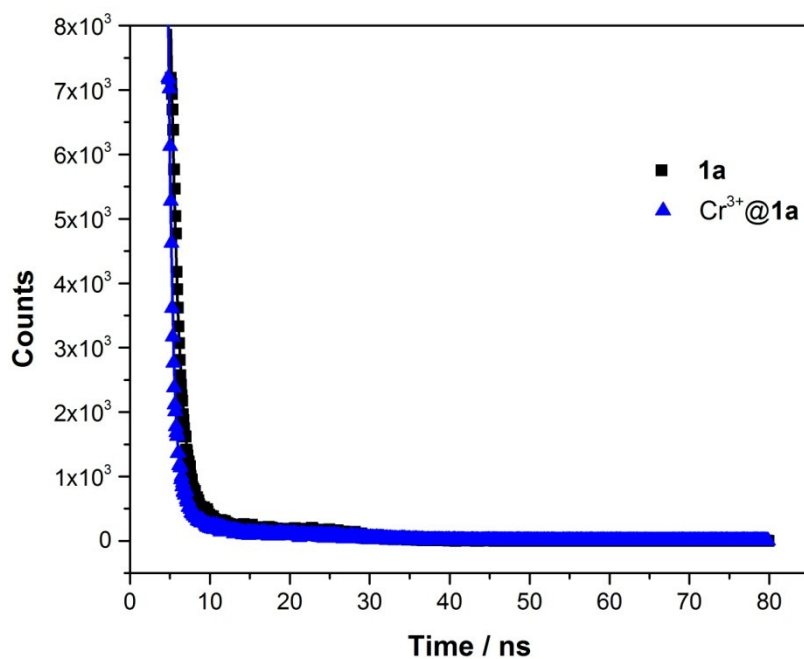


Fig. S5 Fit result of the time-resolved fluorescence decay traces of **1a** and Cr^{3+} @**1a**.

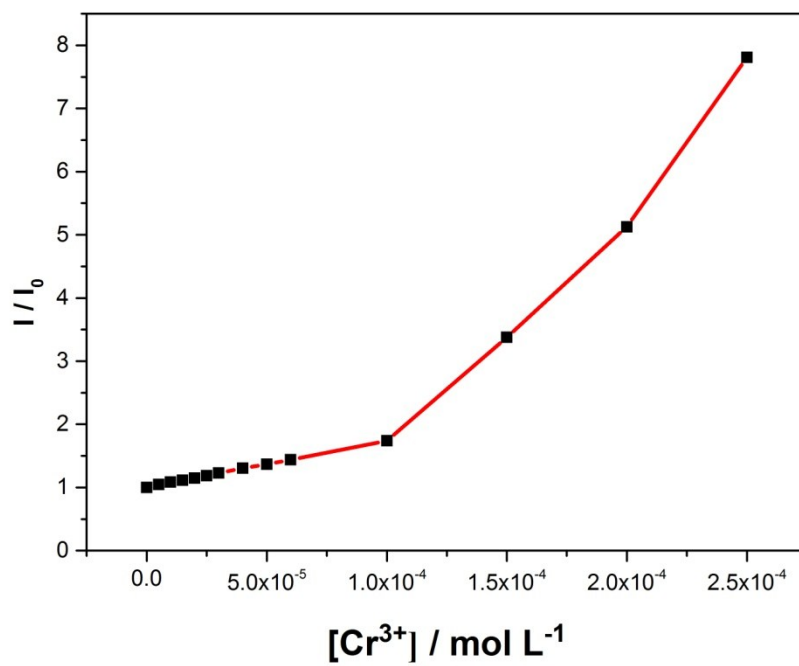


Fig. S6 The I_0/I versus the concentration of Cr^{3+} ion for **1a** (from 0 to 0.25 mM).

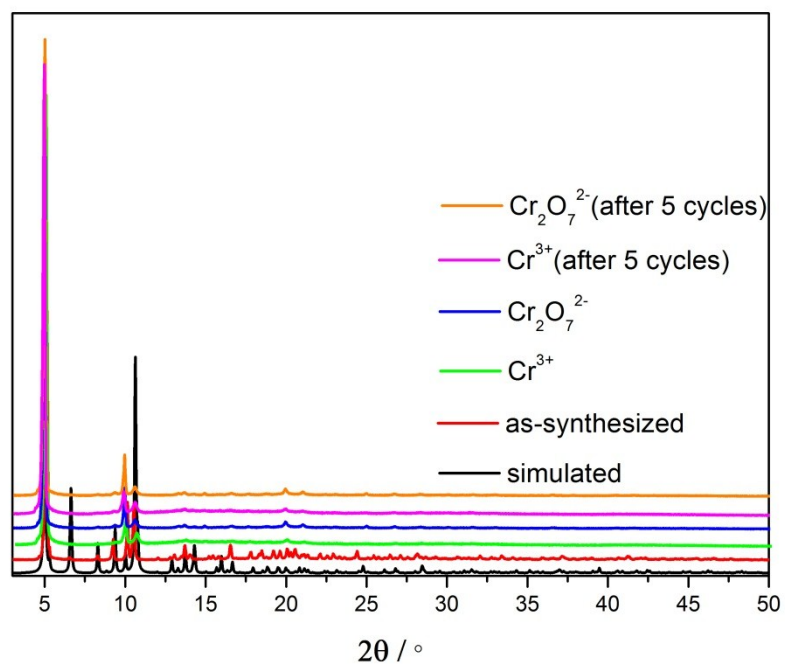


Fig. S7 PXR D patterns of simulated, the as-synthesized, $\text{Cr}^{3+}@1\mathbf{a}$, $\text{Cr}_2\text{O}_7^{2-}@1\mathbf{a}$, Cr^{3+} (after 5 cycles) and $\text{Cr}_2\text{O}_7^{2-}$ (after 5 cycles).

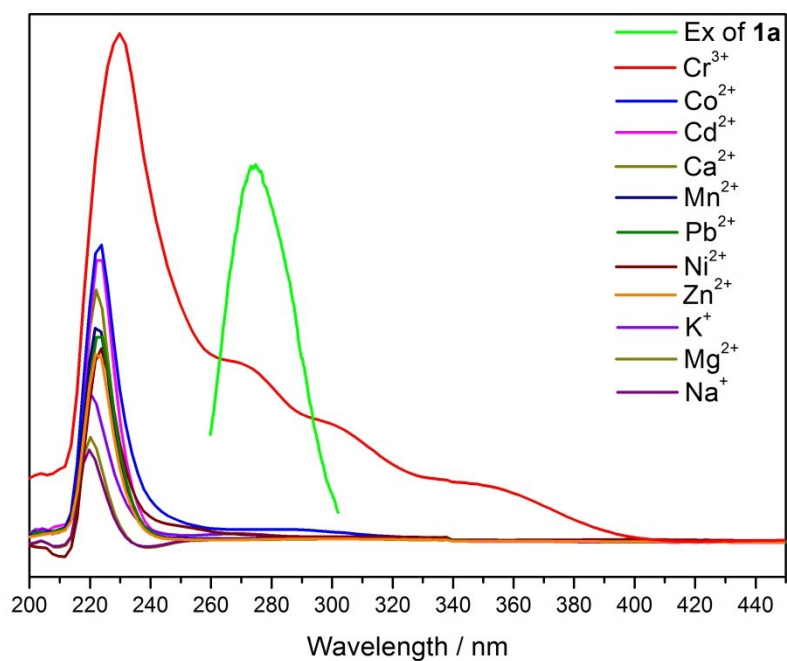


Fig. S8 UV-Vis adsorption spectrum of $\text{M}(\text{NO}_3)_n$ aqueous solution and the excitation spectrum of 1a.

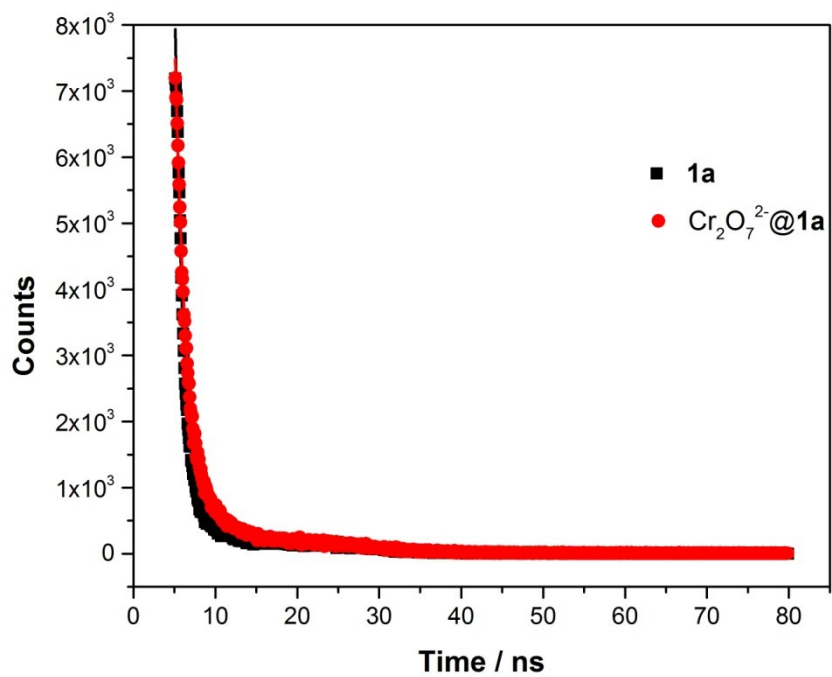


Fig. S9 Fit result of the time-resolved fluorescence decay traces of **1a** and Cr₂O₇²⁻@**1a**.

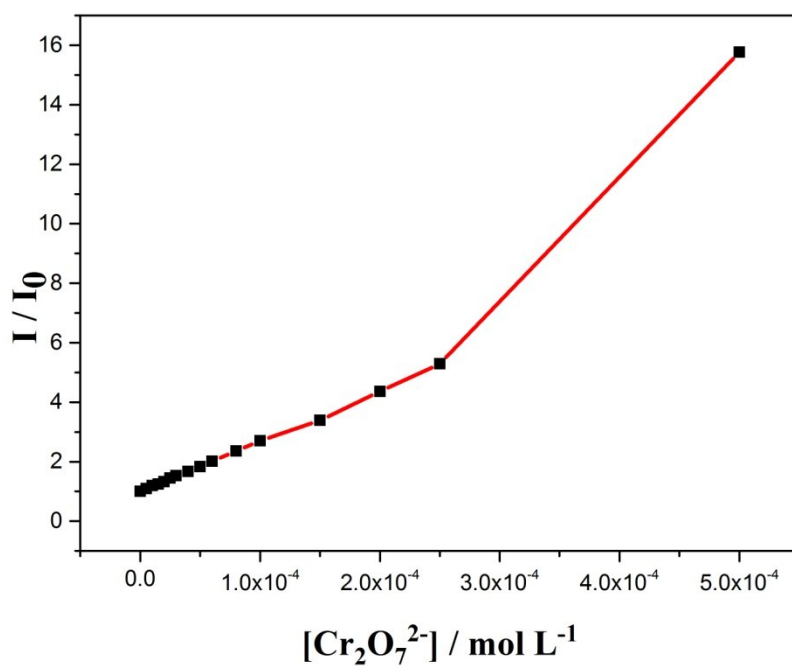


Fig. S10 The I_0/I versus the concentration of Cr₂O₇²⁻ ion for **1a** (from 0 to 0.5 mM).

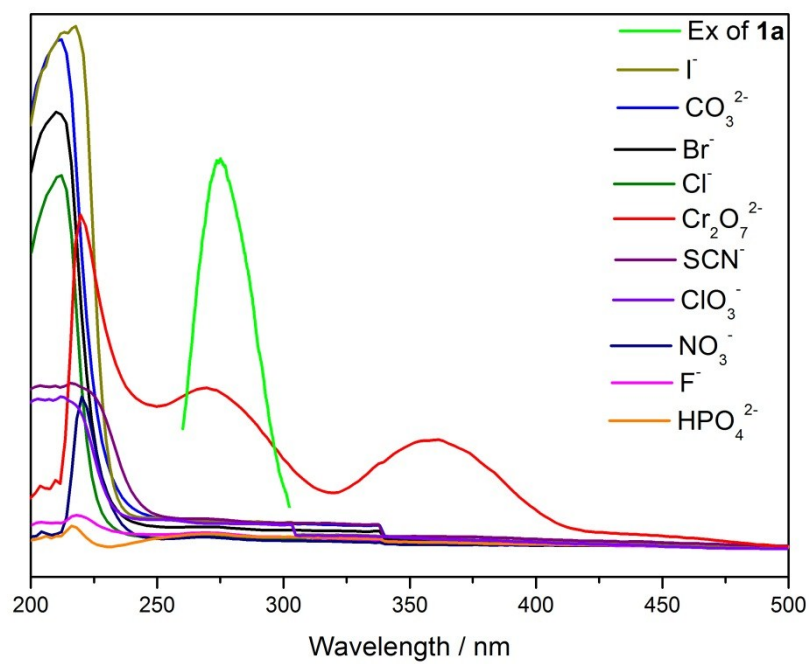


Fig. S11 UV-Vis adsorption spectrum of $K_{11}(A)$ aqueous solution and the excitation spectrum of **1a**.